

Parametric influences on the flyer velocity driven by electrical explosion

Qingchou Chen^{*}, Tao Ma^{*}, and Yong Li^{*†}

^{*}Institute of Chemical Materials, China Academy of Engineering Physics,
No. 64 Mianshan Road, Mianyang 621999, CHINA
Phone: +86-816-2494300

[†]Corresponding author: liyong_icm@caep.cn

Received: June 25, 2018 Accepted: February 6, 2019

Abstract

As the crucial qualification of the exploding foil initiators (EFIs) initiation, the velocity of the flyer driven electrical explosion is tended to measure and calculate accurately. The electrical performance tests were conducted to measure the current and voltage histories of the metal foils, which can scale the electrical energy absorbed into the metal foil. The burst time delays and the burst current increases as the width and the thickness of the metal foil increase. The size effects on the burst current and the burst time appear in a linear relationship at certain charging voltages. An available Photonic Doppler Velocimetry (PDV) system was conducted to measure the actual velocity of the flyer driven by electrical explosion. The velocity histories of the flyer were obtained in different parameters of the metal foil, flyer and barrel. The two-phase acceleration is presented due to different dynamical mechanisms, which are shock driving mainly at first and expansion driving latter. The effect of the foil width and flyer velocity on the flyer velocity is evidently, while the effect of foil thickness is slight relatively. One-dimensional Lagrange hydrodynamic calculations were carried out to compare with the experimental data, which reveals good agreement. The correction factor was determined by matching the calculated curve to the experimental one. The calculation method can be used to predict the acceleration process of the flyer driven by electrical explosion.

Keywords: exploding foil initiators, electrically explosion, flyer velocity, Photonic Doppler Velocimetry

1. Introduction

Exploding foil initiators (EFIs) are a kind of third generation pyrotechnic devices, of whom the behavior has been studied extensively for detonator applications in fuze system. As a main feature of the in-line electrical fuze, EFIs advance in the safety of the warhead and even the weapon system. The concept of accelerating plate by exploding foils was first formulated by Keller¹⁾ and Guenther²⁾ at 1962. Based on this technique, Stroud proposed the frame of EFIs and applied the patent of it at 1965³⁾.

For the development of EFIs the following topics are of interest: the electrical circuit, the exploding foil, the velocity of the flyer, the explosive pellet⁴⁾. In order to calculate the energy transition and the flyer velocity for EFI, the measurements of burst current and voltage for the electrical explosion of metal foil were carried out

experimentally⁵⁾⁻⁷⁾. The dynamic conductivity models of metal foil were built and used for the numerical simulations of electrical explosion⁸⁾⁻¹⁰⁾. As the key factor of initiation, measurements of the flyer velocity were undertaken since the 1980s. The measurements of average velocity were carried out at the beginning of EFIs investigation¹¹⁾. Because of the absence of the exact velocity at the impact, the velocity history needs to obtain. The flyer velocity histories achieved by velocity interferometer system for any reflector (VISAR) in 1991¹²⁾. However, the treatments of the flyer surface have to achieve in many ways to get a diffuse reflection¹²⁾, which change the state of flyer and increase the mass of the flyer. Photonic Doppler Velocimetry (PDV)¹³⁾ becomes a primary diagnostics of EFIs recently due to no need of the treatment of the flyer surface. The velocity measurements of flyer driven by electrical explosion have achieved by

PDV^{14,15}). In order to have a better understanding of electrical explosion driving flyer, calculation models were built to calculate the velocity. Electrical gurney model have been developed to calculate the final velocity¹⁶, and amended to temporal velocity¹⁷. One-dimension Lagrange hydrodynamic model¹⁸ and three-dimensional magneto-hydrodynamic analysis¹⁹ of EFIs were carried out to provide additional insight into optimizing the design of such devices.

In this paper, the current and voltage histories of metal foil were measured and calculated for the energy balance in calculations of the flyer velocity. The actual velocities of flyers driven by electrical explosion were obtained by PDV diagnostic. The effects of the foil width, the foil thickness and the flyer thickness on the flyer velocity were investigated. Numerical calculations were presented, which can predict the flyer velocity on some conditions.

2. Experimental techniques

2.1 Electrical performance tests

The burst current is defined as the current at the time of maximum voltage in an electrical explosion process²⁰. The burst time used in this paper is the time at maximum voltage. The burst current and time could indicate the respond of the metal foil at the stimulation of current pulse. Also, the electrical energy need quantitate for the investigation of flyer driving process.

The current and the voltage histories of electrical explosion process are measured by a Rogowski coil and a Voltage probe in the discharging circuit. The simplified schematic diagram of the discharging circuit is illustrated in Figure 1, which generates a specific current pulse to stimulate the metal foil.

The DC source charges up the capacitor firstly. When the switch closed, the subsequent current pulse stimulates the metal foil to explode electrically. The current and the voltage on the metal foil are non-linear relationship because of the dynamic resistivity of the metal foil. The Rogowski coil is a most popular means to record the current history, which is based on electromagnetic induction techniques. The voltage of the metal foil is measured accurately by a voltage probe connected to the both electrodes.

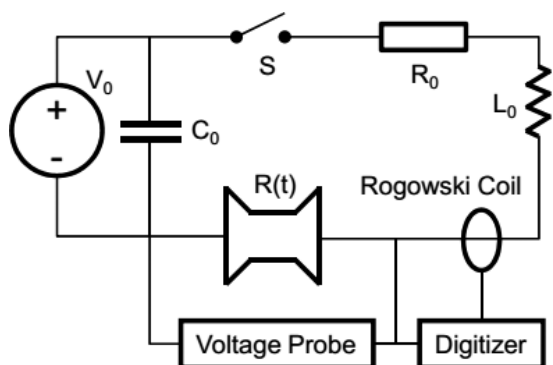


Figure 1 Simplified schematic diagram of the discharging circuit.

2.2 Flyer velocity measurement

The velocities of flyer driven by electrical explosion were measured using an available PDV system. The scheme of experimental apparatus is illustrated in Figure 2 below. As a current pulse stimulated, the metal foil explodes instantly and vaporizes into plasma. The flyer is formed due to the high-pressure plasma expanding and accelerates to a high velocity. The moving flyer reflects the laser light into the probe with the information of Doppler frequency shift. A beat signal is detected and records by a digitizer.

PDV is a displacement interferometer based upon the heterodyne technique. A probe containing a lens is used to launch the laser light onto the moving surface and collect a reasonable amount of the light reflected or scattered from the moving surface. The collected Doppler-shifted light is transported by fiber to the detector. By a circulator, a fraction of the light emitted by the laser is transported by fiber directly to the detector without being Doppler shifted. Such a scheme is shown conceptually in the following Figure 3¹³.

Showed in the scheme, the frequency of the light of the laser is f_0 , and the frequency of the Doppler-shifted light is f_d . The beat signal is generated at the detector with a frequency f_b equal to the difference between the Doppler-shifted frequency f_d and the un-shifted frequency f_0 . The beat frequency is given by Equation (1).

$$f_b = f_d - f_0 = 2\left(\frac{u}{c}\right)f_0 \quad (1)$$

With the speed of light $c = f_0\lambda_0$, where λ_0 is the

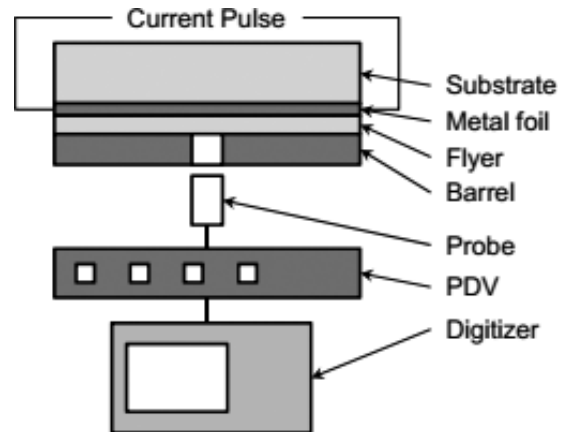


Figure 2 Scheme of velocity measurement system of the flyer driven by electrical explosion.

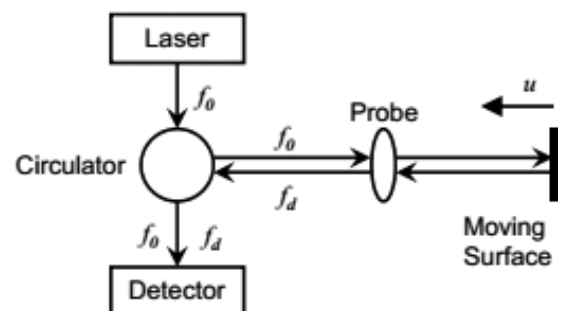


Figure 3 Simplified schematic diagram of PDV.

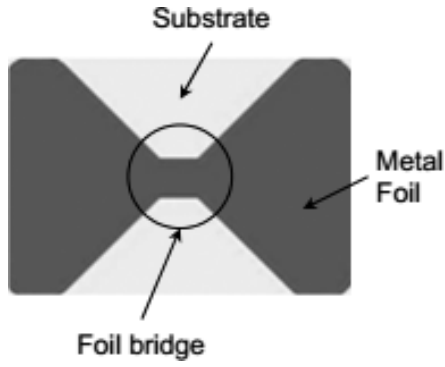


Figure 4 Schematic diagram of the metal foil shape.

Table 1 The parameters of the copper foils, the flyers and the barrels.

Type	w_{foil} [mm]	h_{foil} [μm]	d_{barrel} [mm]	h_{flyer} [μm]
1	0.2	3	0.30	25
2	0.3	3	0.45	13
3	0.3	3	0.45	25
4	0.3	3	0.45	50
5	0.4	3	0.60	25
6	0.4	4	0.60	25

Note: w_{foil} , h_{foil} , d_{barrel} and h_{flyer} stand for the width of foil bridge, the thickness of foil bridge, the diameter of barrel and the thickness of flyer.

wavelength emitted by the laser, the velocity is given by Equation (2).

$$u = \left(\frac{\lambda_0}{2}\right) f_b \quad (2)$$

The available PDV system utilizes the Agilent MSO-X 93204A digitizer, which has 32 GHz analog bandwidth. The laser model is the Koheras ADJUSTIK E15 and operates at 1550 nm. The PDV system was designed and manufactured by Nanjing University of Science and Technology.

The copper foils are same as the ones used in the electrical explosion tests. Flyer is made from Kapton polyimide (PI) film. Barrel is manufactured from steel. Velocity measurements of flyer driven by electrical explosion were carried out at same charging voltage.

2.3 Experimental setup

Copper foils were magnetron sputtered onto a porcelain substrate. The magnetron sputter deposition was performed in an evacuated chamber pumped to a base pressure of about 10^{-4} Pa. The atmosphere of the chamber was filled with an inert argon gas so as to initiate the sputtering process. Atoms of copper were sputtered from the target, pure copper (99.99%). The rotating substrate, which receives the plasma resulting in forming films, was positioned directly above the magnetron sources. The metal foils were etched to a specific bow shape functioned as electrodes and exploding foil bridge, which showed in Figure 4.

The size of the metal foil bridge is denoted by width and thickness. Four sizes of the metal foils are used in

electrical performance tests. Six combinations of the copper foil, flyer and barrel are used in flyer velocity measurements, which were assembled together. The parameters of the copper foil, flyer and barrel are listed in Table 1.

The diameter of barrel is dependent on the width of foil bridge, which is 1.5 times as long as the width of foil bridge. So the effect of the diameter of barrel is not considered in this paper. For the particular discharging circuit used, C_0 is 0.20 μF , R_0 is 175 m Ω , L_0 is 240 nH. The charging voltages are 2.8 kV and 3.4 kV in the electrical performance tests, and 2.8 kV in the flyer velocity measurements.

3. Calculation method

3.1 Electrical performance modelling

The discharging circuit is a typical resistor-inductor-capacitor (RCL) circuit, which can be expressed by Equation (3) below:

$$L \frac{dI}{dt} + I(R_0 + R(t)) + \frac{1}{C_0} \left(\int_0^t Idt + Q_0 \right) = 0 \quad (3)$$

where: C_0 is capacitance, L_0 is inductance, R_0 is static resistance, V_0 is charging voltage of the capacitor, $I(t)$ is current, $R(t)$ is the dynamic resistivity of the metal foil.

The dynamic conductivity can be described by the model presented by Zhao⁸⁾. The model characterizes the electrical explosion as three phases:

1) Joule heat phase

At the Joule heat phase, the expansion of the metal foil is unconsidered. The physical state can be described by temperature. The conductivity of metal foil reduces as temperature increases at a large range. The conductivity expressed by Equation (4) in the phase:

$$\sigma = \sigma_0 [1 + \alpha(T - T_0)]^{-1} \quad T \leq 3000 \text{ K} \quad (4)$$

where σ_0 is the conductivity at temperature T_0 , α is the coefficient which depends on temperature.

2) Latent explosion phase

At the latent explosion phase, the metal foil begins to gasify. The resistance of the metal foil increases rapidly until the electrical explosion occurs. This feature of the resistance makes the current falls down and the voltage increases distinctly. The conductivity expressed by Equation (5) in the phase.

$$\sigma = \frac{n_e}{n_a^2 \gamma_v z T} \quad 3000 \text{ K} < T \leq 8000 \text{ K} \quad (5)$$

where n_e is electron density, n_a is atom density, z is ion equivalent charge, γ_v is the ratio of volume expansion coefficient and specific thermal capacity.

3) Plasma phase

At the continuous effect of the current, the plasma generates due to the ionization of metal gasification. The resistance reduces subsequently. The Lee-More model²¹⁾ for dense plasma is suitable at this phase:

$$\sigma = (n_e e^2 \tau / m_e) A^\alpha (\mu / kT) \quad 8000 \text{ K} < T \quad (6)$$

When the dynamic conductivity of the metal foil is

introduced, the current $I(t)$ can be calculated by solving Equation (3) numerically. The voltage $V(t)$ and the electrical power $P(t)$ can be obtained by $I(t)$ and $R(t)$.

3.2 Flyer velocity modelling

The electrical explosion of metal foil occurs simultaneously with the energy dissipation in the forms of light, heat and electromagnetic wave, also with inner energy of materials increased. On that condition, the electrical energy absorbed by metal foil cannot fully convert to kinetic energy of flyer. The specific power $PP(t)$ is used to present the electrical energy converted to flyer motion. Because the energy dissipation is difficult to describe accurately, an empirical coefficient named correction factor β is conducted to characterize the conversion⁸⁾, which defined by Equation (7).

$$PP(t) = \beta \left(\frac{P(t)}{m_b + m_f} \right) \quad (7)$$

where m_b and m_f are the mass of metal foil and flyer respectively. As the significant state change of metal foil after electrical explosion, it is reasonable that the correction factor varies after burst. So β presents separately in Equation (5).

$$\beta = \begin{cases} \beta_1 & \beta_1 \leq t_b \\ \beta_2 & \beta_2 > t_b \end{cases} \quad (8)$$

where t_b is burst time.

The physical model of flyer movement can be abstracted from flyer driven by electrical explosion under the following suppositions: a) the factors of expansion, melt and gasification of the metal foil are not considered in modeling states of solid-liquid phase by hydrodynamic Equations. Heats of melt and gasification of the metal foil are considered in describing states of liquid-plasma phase by Equation of state. b) the thickness of the metal foil is rather small and only several microns, which is less than the skin depth of the current. Therefore, joule heat is uniformly distributed in the metal foil. c) Strength effects, heat conduction and two-dimensional side effects in quickly acceleration process and short time duration are ignored at the condition of high pressure plasma. The flyer moves as ideal fluid. Therefore, it can be considered as one-dimensional planar non-steady compressible fluid. d) Substrate is treated as a rigid body, because the mass of substrate is far bigger than flyer.

On the condition of the assumptions above, the flyer movement process could be described by one-dimensional Lagrange planar compressible hydrodynamic Equations (9)–(13).

Conservation of mass:

$$\frac{\partial \rho}{\partial x_0} + \nabla(\rho u) = 0 \quad (9)$$

Conservation of momentum:

$$\rho \frac{du}{dy} + \nabla(p + q) = 0 \quad (10)$$

Conservation of energy:

$$\rho \frac{de}{dt} = -(p + q) \nabla u + PP(t) \quad (11)$$

Movement Equation

$$\frac{dx}{dt} = u \quad (12)$$

Equation of state

$$p = C_0^2(\rho - \rho_0) + (\gamma - 1)e\rho \quad (13)$$

where p , ρ , e , u and x are pressure, density, specific internal energy, coordinate and velocity. γ is adiabatic coefficient. q is pseudo-viscosity, which is defined as the Equation (14).

$$q = \begin{cases} \rho [a_1 \left| \frac{\partial u}{\partial x} \right| + a_s^2 \left| \frac{\partial u}{\partial x} \right|^2] \frac{\partial u}{\partial x} < 0 \\ 0 & \frac{\partial u}{\partial x} \geq 0 \end{cases} \quad (14)$$

where p , ρ , e , u and x are pressure, density, specific internal energy, coordinate and velocity. γ is adiabatic coefficient. q is pseudo-viscosity.

Boundary conditions are considered in the calculation. The velocity, pressure and specific internal energy of exploding foil and the velocity of flyer are all zero at initial time. The substrate is considered as a rigid body. The interface between substrate and exploding foil is fixed. The velocity and the pressure at interface between exploding foil and flyer are continuous. Meanwhile the other side of flyer is free surface.

Using the data of $P(t)$ obtained in the former section, the flyer velocity could be calculated by the resolution of Equations (9)–(13).

4. Results and discussion

4.1 Electrical performance

The parameters of the discharging circuit, the metal foils, the flyers and the barrels are presented in the section of experimental set, which be used as input to the calculation schemes.

Several electrical performance tests were employed at different charging voltage. The calculations of the current and the voltage on metal foils were at same conditions. The comparisons of the experimental and calculated data at 3.4 kV are enumerated in Figure 5.

The comparisons results show that the calculations of the current and the voltage histories have great agreement with the experimental ones. The varying tendency of voltage implies the dynamic conductivity at different phase. The burst time delays as the width and the thickness of the metal foil increases. The burst time of the foil with 0.4 mm width and 4 μm thickness is most near the peak of current waveform, which represents the sufficient energy supply and high efficiency of the circuit.

Figure 6 illustrates the burst currents and the burst times of different size foil at different charging voltage.

The size effects on the burst current and the burst time appear in a linear relationship at certain charging voltages. The electrical explosion concerns the current density

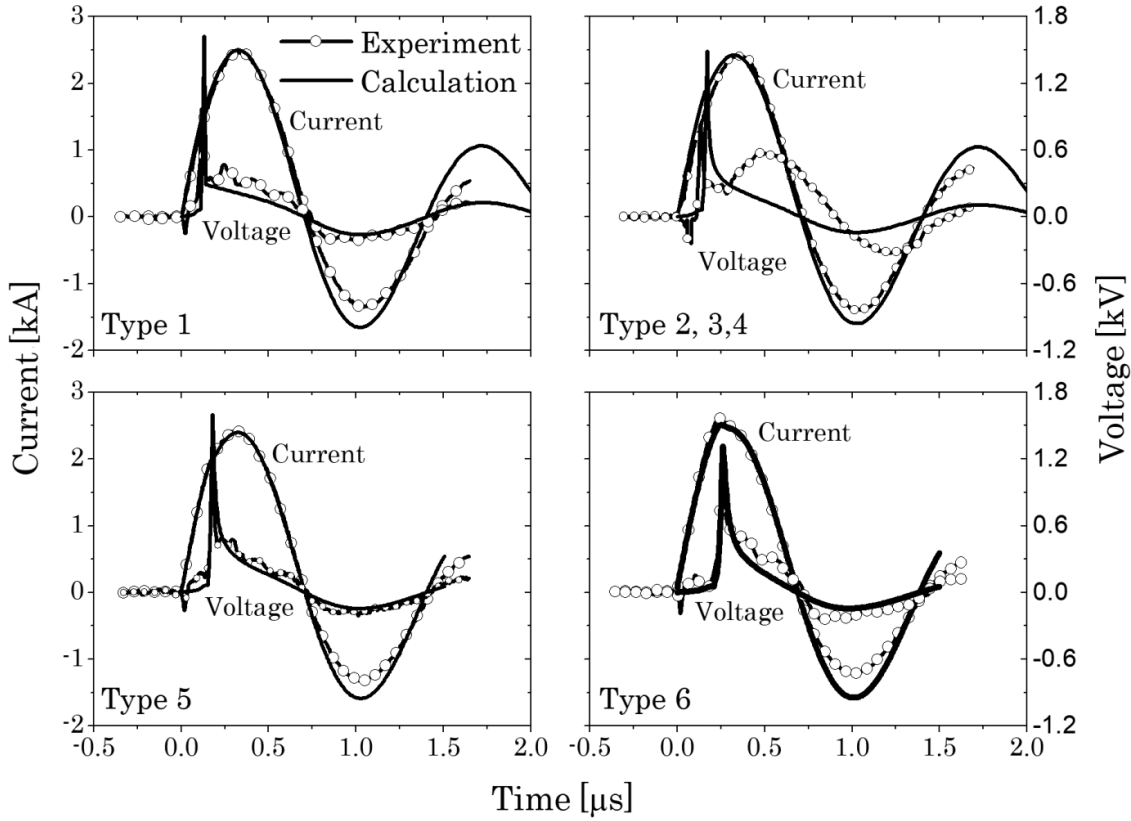


Figure 5 The comparisons of the experimental and calculated current and voltage at 3.4 kV.

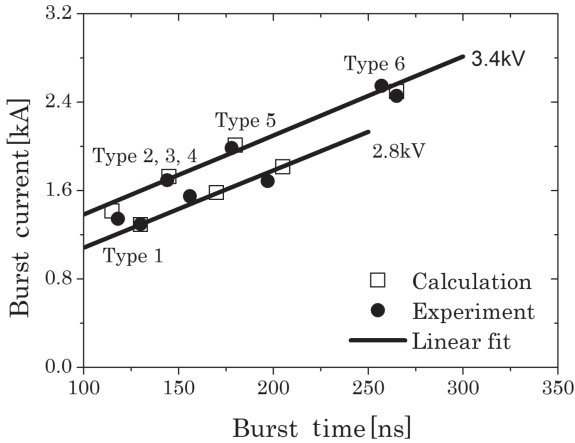


Figure 6 The size effects on the electrical performance.

extremely. Considering same charging voltage, the current density depends on the section area of metal foil simply.

4.2 Flyer velocity

In the one-dimensional discussion, metal foil is restricted by substrate and flyer. The thermal properties of the porcelain substrate and PI flyer are invariable, and substrate was treated as a rigid body in the calculation. These conditions make the flyer thickness as the only factor of the energy conversion. So the correction factor depends on the flyer thickness mainly in our one-dimensional calculation.

According to the experimental data of the Type 1 test, the corresponding calculation was performed. The correction factor was adjusted to match the calculated curve for the experimental one. On the condition of the

Table 2 Correction factors used in the calculations.

Type	Flyer thickness [μm]	β_1	β_2
2	13	0.1	1.0
1, 3, 5, 6	25	0.2	1.5
4	50	0.5	2.7

consistency, the correction factors are determined for 25 μm flyer. Then, the correction factors were used in other calculations with the same flyer thickness. The same procedures were carried out for the rest thickness. The correction factors at the conditions of different flyer thickness are listed in Table 2.

All the comparisons of the flyer velocities between experimental and calculation are showed in Figure 7. All the comparisons results show that the calculations of velocity histories have great agreement with the experimental ones.

The history of flyer velocity has two stages of acceleration process apparently. At earlier stage, the flyer velocity is going up sharply. Usually it only takes less than 100 ns, while the 75% acceleration is finished in this stage. At latter stage, the flyer velocity is going up smoothly relatively and keeping increase for several hundred nanoseconds.

According the two phase acceleration, different dynamical mechanism is operated. At first stage, the stimulation of the current pulse makes the inner energy and concomitant pressure of copper foil increase very high. The aggressive compression to flyer of this high pressure generates a shock wave conceivably, which

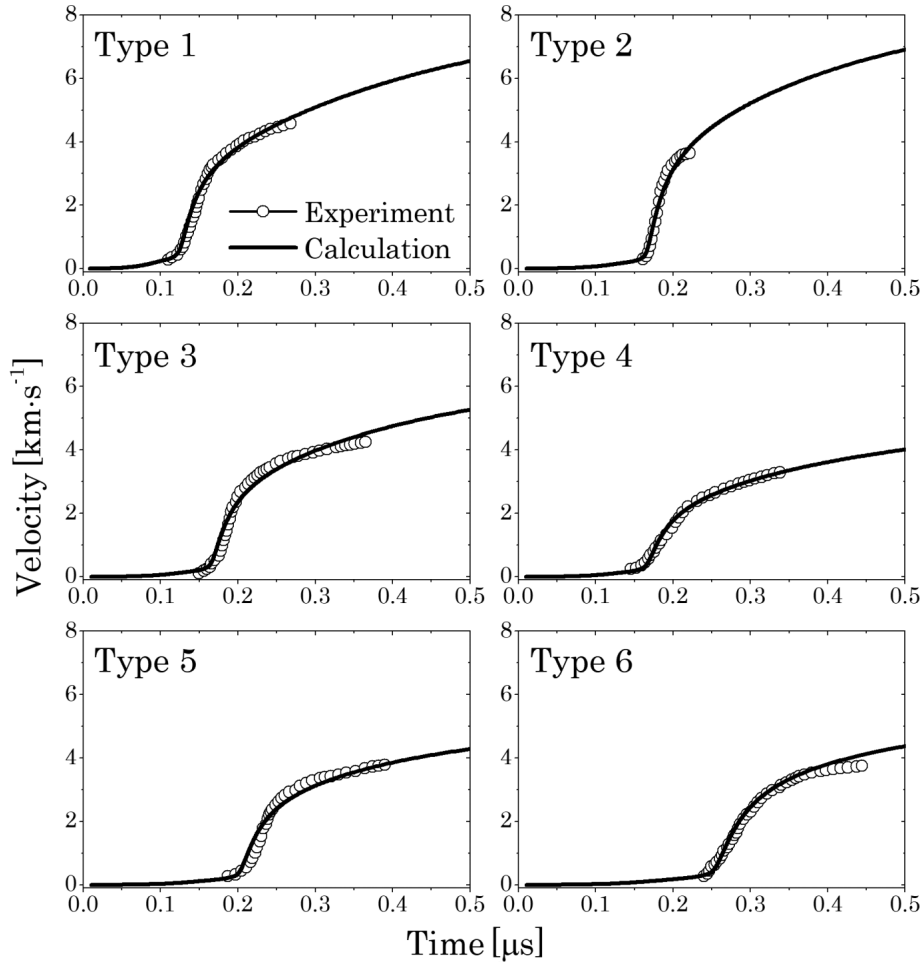


Figure 7 Comparisons of the flyer velocities driven by electrical explosion at 2.8 kV.

makes the flyer accelerate sharply. Schlieren visualizations of Shock induced by electrical explosion have been observed in the detonator investigations²²). At second stage, the electrical explosion produces quantitative plasma, which expands and drives the flyer. The expansion velocity of the plasma is slow relatively, which makes the second stage of the velocity history flat.

The accurate velocity of flyer impacted on the explosive pellet is important to predict the behaviour of EFIs initiation. As the flyer moving, the impact velocity depends on the barrel length or the displacement of the flyer. So the velocities at some certain displacements of the flyer motion are concerned. From the analysis of two phase acceleration, 0.2 mm is long enough to finish the first stage of acceleration. Another empirical displacement of 0.4 mm is chosen comparatively. Figure 8 shows the effect of the foil width on the flyer velocity at different displacement of flyer motion. The foil widths of 0.2 mm, 0.3 mm, 0.4 mm and 0.5 mm are considered.

From the Figure 8, the flyer velocity at 0.2 mm displacement or 0.4 mm reduces about 10% as the foil width increases every 0.1 mm. At the certain foil width, the flyer velocity increases about 15% as the flyer displacement from 0.2 mm to 0.4 mm. The result indicates that reducing the foil width can increase the flyer velocity efficiently.

Figure 9 shows the effect of the foil thickness on the flyer velocity at different displacement of flyer motion.

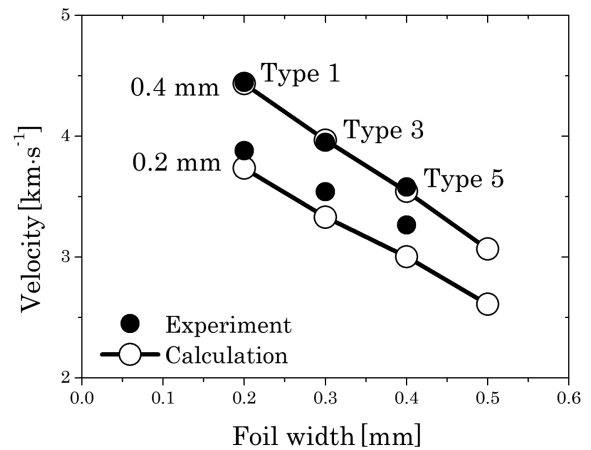


Figure 8 Effect of the foil width on the flyer velocity at 2.8 kV.

The foil thicknesses of 3 μm , 3.5 μm , 4 μm , 4.5 μm , and 5 μm are considered.

From the Figure 9, the flyer velocity at 0.2 mm displacement or 0.4 mm increases slowly as the foil thickness increases. The velocities vary less than 6% from 3 μm to 5 μm foil thickness at the same displacement of the flyer. For the certain foil thickness, the flyer velocity increases about 18% as the flyer displacement from 0.2 mm to 0.4 mm. The result indicates that the foil thickness barely has influence on the flyer velocity.

Figure 10 shows the effect of the flyer thickness on the flyer velocity at different displacement of flyer motion.

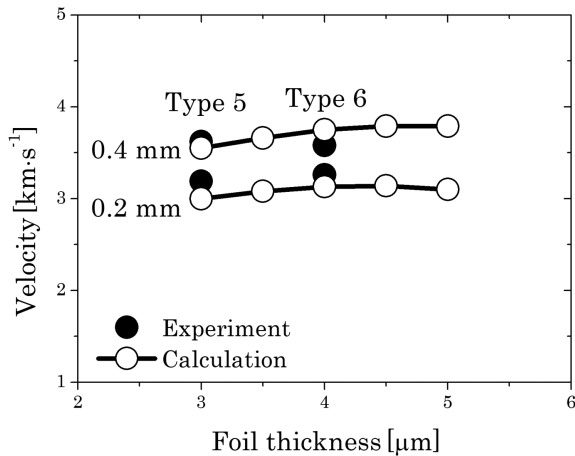


Figure 9 Effect of the foil thickness on the flyer velocity at 2.8kV.

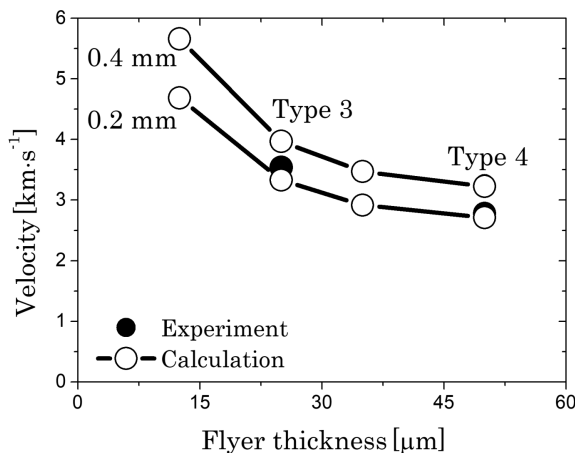


Figure 10 Effect of the flyer thickness on the flyer velocity at 2.8kV.

The flyer thicknesses of 13 μm , 25 μm , 38 μm and 50 μm are considered.

From the Figure 10, the flyer velocity at 0.2mm displacement or 0.4mm reduces exponentially as the flyer thickness increases. The velocities vary sharply when the flyer thickness increase from 13 μm to 25 μm , while smoothly after 25 μm . At the certain foil thickness, the flyer velocity increases about 15% as the flyer displacement from 0.2mm to 0.4mm. The result indicates that the foil width have few influence on the flyer velocity.

5. Conclusions

The electrical performance tests were conducted to measure the current and voltage histories of the metal foils, which can scale the electrical energy absorbed into the metal foil. The burst time delays and the burst current increases as the width and the thickness of the metal foil increase. The size effects on the burst current and the burst time appear in a linear relationship at certain charging voltages. Using the dynamic conductivity model, the current and voltage histories can be calculated precisely.

The actual velocities of the flyer driven by electrical explosion were investigated by the PDV diagnostic. The velocity histories of the flyer were obtained in different parameters of the metal foil, flyer and barrel. The two-phase acceleration is presented due to different dynamical

mechanisms, which are shock driving mainly at first and expansion driving latter. The effect of the foil width and flyer velocity on the flyer velocity is evidently, while the effect of foil thickness is slight relatively. One-dimensional Lagrange hydrodynamic calculations were carried out to compare with the experimental data, which reveals good agreement. The calculation method can be used to predict the acceleration process of the flyer driven by electrical explosion.

References

- 1) D. V. Keller and R. J. Penning, Proc. Second Conference on the Exploding Wire, New York, USA (1962).
- 2) A. H. Guenther, D. C. Wunsch, and T. D. Soapes, Proc. Second Conference on the Exploding Wire, New York, USA (1962).
- 3) J. R. Stroud, A new kind of detonator — the Slapper, Report UCRL-7739, Lawrence Livermore National Laboratory, Livermore, CA, USA (1976).
- 4) W. C. Prinse, P. G. Van't Hof, and L. K. Cheng, 27th International congress on High-Speed Photography and Photonics, International Society for Optics and Photonics, Xi'an China (2007).
- 5) C. Xu, P. Zhu, K. Chen, W. Zhang, R. Shen, and Y. Ye, IEEE Electron Device Lett., 38, 1610–1613 (2017).
- 6) J. Wu, L. Wang, Y. Li, L. YANG, M. Sultan, and L. Chen, Plasma Sci. & Technol., 20, 075501 (2018).
- 7) P. Zhu, K. Chen, C. Xu, S. Zhao, R. Shen, and Y. Ye. Sens. Actuators, A, 276, 278–283 (2018).
- 8) Y. Zhao, Q. Zeng, and C. Feng, J. Beijing Inst. Technol., 19, 8–12 (2010).
- 9) B. Luo, C. Sun, J. Zhao, and J. He, IEEE Trans. Plasma Sci., 41, 49–57 (2013).
- 10) Y. Wang, X. Sun, H. Jiang, Y. Gao, F. Guo, L. Wang, Y. Zhang, and Q. Fu, Propellants, Explos., Pyrotech., 43, 923–928 (2018).
- 11) J. A. Waschl and D. J. Hatt, Int. J. Impact Engng., 14, 785–796 (1988).
- 12) D. J. Hatt, Report MRL-TR-91-42, Materials Research Laboratory, Ascot Vale, Australia (1991).
- 13) O. T. Strand, L. V. Berzins, and D. R. Goosman, Velocimetry Using Heterodyne Techniques, Report UCRL-CONF-206034, Lawrence Livermore National Laboratory, California, USA (2004).
- 14) R. Hodgkin, C. May, and R. Hanks, Report UCRL-CONF-230794, Lawrence Livermore National Laboratory, California, USA (2007).
- 15) Q. Chen, L. Chen, W. Qin, F. Guo, and Z. Han, Chin. J. Energ. Mater., 22, 413–416 (2014).
- 16) T. J. Tucker and P. L. Stanton, Report SAND-75-0244, Sandia National Laboratories, Albuquerque, USA (1975).
- 17) S. C. Schmidt, W. L. Seitz, and J. Wackerle, Report LA-6809, Los Alamos National Laboratory, NM, USA (1977).
- 18) L. Liang, Z. Fan, and X. Hu, Acta Armamentarii, 20, 102–107 (1999).
- 19) J. S. Christensen and C. A. Hrousis, Report DE-AC52-07NA 27344, Lawrence Livermore National Laboratory, California, USA (2010).
- 20) T. J. Tucker, Exploding Wires, 3, 175–178 (1964).
- 21) Y. T. Lee and R. M. More, Phys. Fluids, 27, 1273–1286 (1984).
- 22) M. J. Murphy and R. J. Adrian, Exp. Fluids, 43, 163–171 (2007).